Effective detection of spatio-temporal carrier dynamics by carrier capture

Journal of Physics: Condensed Matter

LETTER • **OPEN ACCESS**

Effective detection of spatio-temporal carrier dynamics by carrier capture

To cite this article: R Rosati *et al* 2019 *J. Phys.: Condens. Matter* **31** 28LT01

OPEN ACCESS
IOP Publishing

Letters
Journal of Physics: Condensed Matter

J. Phys.: Condens. Matter **31** (2019) 28LT01 (6pp)
https://doi.org/10.1088/1361-648X/ab17a8

Letter

Effective detection of spatio-temporal carrier dynamics by carrier capture

R Rosati[1,2], **F Lengers**[1], **D E Reiter**[1] and **T Kuhn**[1]

[1] Institut für Festkörpertheorie, Universität Münster, Wilhelm-Klemm-Str. 10, 48149 Münster, Germany
[2] Department of Physics, Chalmers University of Technology, SE-412 96 Gothenburg, Sweden

E-mail: roberto.rosati@chalmers.se

Received 11 February 2019, revised 28 March 2019
Accepted for publication 9 April 2019
Published 26 April 2019

Abstract

The spatio-temporal dynamics of electrons moving in a 2D plane is challenging to detect when the required resolution shrinks simultaneously to nanometer length and subpicosecond time scale. We propose a detection scheme relying on phonon-induced carrier capture from 2D unbound states into the bound states of an embedded quantum dot. This capture process happens locally and here we explore if this locality is sufficient to use the carrier capture process as detection of the ultrafast diffraction of electrons from an obstacle in the 2D plane. As an example we consider an electronic wave packet traveling in a semiconducting monolayer of the transition metal dichalcogenide $MoSe_2$, and we study the scattering-induced dynamics using a single particle Lindblad approach. Our results offer a new way to high resolution detection of the spatio-temporal carrier dynamics.

Keywords: spatio-temporal dynamics, phonon-mediated carrier capture, Lindblad description, high-resolution detection

(Some figures may appear in colour only in the online journal)

1. Introduction

Detecting the spatio-temporal dynamics of generic (quasi-) particles [1–11] is challenging when a subpicosecond temporal scale has to be combined with a nanometer spatial resolution [4, 8]. Nevertheless it is of high interest to unravel the spatio-temporal carrier dynamics to use it, e.g. in quantum information protocols, and several studies have investigated how small wave packets evolve or can be controlled [12–16].

In this paper we propose a mechanism to detect and reveal the spatio-temporal dynamics of an electronic wave packet moving in a semiconducting two-dimensional (2D) system. The detection mechanism relies on the phonon-induced carrier capture [16–29] from the delocalized states in the 2D host material into the bound states of a quasi-zero dimensional quantum dot (QD) embedded in this material. The captured carriers can then recombine on a longer time scale resulting in an optical signal spectrally well separated from the host material's optical signals, providing information on the time-integrated carrier capture into the QD. Using ultrafast pump-probe spectroscopy on a single QD [30, 31], time-resolved information on the QD population, and thus on the capture process, can also be obtained [27]. The crucial aspect for the detection is that the carrier capture happens locally [16, 25–29], i.e. only when the electronic density is close to the QD it can be captured. Here we analyze the question, whether this locality is pronounced enough to describe *where* the electronic wave packet was distributed. In other words, we examine, if the phonon-induced carrier capture can be used to spatially resolve efficiently the ultrafast dynamics of the electronic density.

As a testbed, we will consider the diffraction of an electronic wave packet moving in a monolayer of a transition metal dichalcogenide (TMDC) at an obstacle. TMDCs represent

a class of 2D semiconducting materials which has recently attracted lots of attention [32–38], mostly due to their excitonic properties, although a mixture of bound and unbound electron–hole pairs could be present [39, 40]. In these materials QDs can be created efficiently, e.g. by applying a tensile strain [41–48], resulting in clearly resolved optical signals. Alternatively, a localized attractive potential for a single type of carriers—electrons or holes—can be achieved by applying a strongly localized gate voltage, e.g. by means of a tip of a scanning tunneling microscope. Such tip-induced QDs have already been realized in graphene [49], and tip-induced band-bending effects in $MoSe_2$ monolayers of few tens of meV have been estimated [50]. While QDs result from an attractive localized potential in the monolayer, an obstacle is formed by a repulsive localized potential. For tip-induced potentials this could be reached by reversing the voltage (see, e.g. [51]). Also, a strongly localized compressive strain, which increases the band gap of TMDCs [52, 53], would result in an obstacle for the carriers. When an electronic density travels inside the TMDC monolayer and gets diffracted at such an obstacle, the spatial dynamics can be theoretically calculated exactly in well specified points. We compare this exact quantity with the predictions provided by the proposed carrier-capture detection scheme, which can be experimentally realized. This will give insight in the efficiency of the proposed scheme.

2. Capture-free dynamics

To be specific, we will consider an electronic wave packet moving in a monolayer of $MoSe_2$, which gets diffracted by an obstacle. The resulting spatial distribution evolves in fringes which, in view of their amplitude and separation, may be challenging to address.

The initial state is assumed to be a pure state with wave function $\psi(\mathbf{r}) \propto \sum_{k_x} \exp\left[-(\epsilon_{k_x} - E_0)^2/(2\Delta_E^2)\right] \exp\left[\imath k_x (x - x_{\mathrm{WP}})\right]$. The energy has a Gaussian distribution in x-direction with $\epsilon_{\mathbf{k}}$ being the energy of the electronic eigenstate in the bare monolayer labeled by the 2D wave vector $\mathbf{k} \equiv (k_x, k_y)$, Δ_E is the energy width and E_0 the excess energy. The energies $\epsilon_{\mathbf{k}}$ for TMDC monolayers are essentially parabolic close to the band gap [28]. In the y-direction the wave packet is homogeneous. Taking $E_0 = 26.8$ meV and $\Delta_E = 4$ meV, this results in a spatial charge density $n(\mathbf{r})$ (with $\mathbf{r} \equiv (x, y)$ being the 2D space vector) behaving as a wavefront with initial FWHM of about 40 nm in x-direction. The initial position of the wave packet is given by $x_{\mathrm{WP}} = -50$ nm and we assume the wave packet moves to the right. A sketch of the initial wave packet is seen in figure 1(a) on the left side. Such a wave packet could be considered as the far field of a localized optical excitation [28] induced by, e.g. near-field or plasmonic excitation [30, 54–59] with ultra-fast nano-optics techniques [60].

Along the motion of the wave packet we consider an obstacle resulting in a non-trivial spatio-temporal distribution. The obstacle is modeled by a potential barrier $V_{\mathrm{B}}(\mathbf{r}) = V_{\mathrm{B}}\,\mathrm{sech}\,(|\mathbf{r}|/a_{\mathrm{B}})$ located at the origin. We take

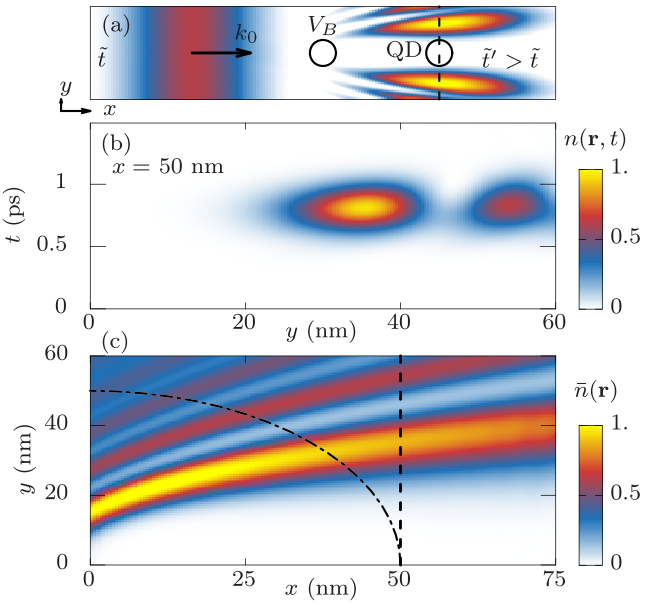

Figure 1. (a) Sketch of the set-up: a wave packet initialized at $t = \tilde{t}$ (left side) impinges on an obstacle V_B resulting in spatial fringes behind the barrier at $\tilde{t}' > \tilde{t}$ (right side). The electronic density might then be detected by a QD. (b) Temporal evolution of the electronic density $n(\mathbf{r}, t)$ at $x = 50$ nm. (c) Time integrated density $\bar{n}(\mathbf{r})$. The dashed and dashed-dotted lines indicate the QD positions probed in figures 2(a) and (b), respectively (note the different scales of the x-and y-axes).

$V_{\mathrm{B}} = 40$ meV as strength of the barrier and $a_{\mathrm{B}} = 5$ nm as its size parameter. After hitting the barrier, the wave packet diffraction leads to fringes with different magnitude and separations as displayed at the right side of figure 1(a). These fringes are on a nanometer scale and we want to explore if our approach is appropriate to resolve them.

In order to understand the timescales, in figure 1(b) we show the temporal evolution of the spatial charge density $n(\mathbf{r}, t)$ along a vertical line at $x = 50$ nm. Note that the electronic density is normalized to its maximal value. We find that the charge is different from zero only in a small time window centered around a time $t_0 \approx 800$ fs and with a width τ of about 300 fs. The time τ quantifies how long the wave packet stays at a given point $\mathbf{r}$, i.e. the duration of the spatio-temporal dynamics we want to study. Its value indicates that this happens on a (strong) sub-picosecond timescale.

Although the spatio-temporal dynamics takes place on an ultrafast timescale, its memory is included in the time-integrated density $\bar{n}(\mathbf{r})$ defined as

$$\bar{n}(\mathbf{r}) = \int_0^{T \gg t_0 + \tau} \mathrm{d}t\; n(\mathbf{r}, t), \tag{1}$$

where we integrate up to a time T being much larger than $t_0 + \tau$. The time-integrated density can be interpreted as the amount of charge which has crossed point $\mathbf{r}$. We show $\bar{n}(\mathbf{r})$ in figure 1(c). We find that the time-integrated density $\bar{n}(\mathbf{r})$ displays the non-trivial spatial behavior of the fringes in agreement with typical wave packet dynamics known, e.g. from light waves.

3. Detection via carrier capture

Now we want to explore if the carrier capture into a QD is able to resolve such nanometer-scale diffraction patterns. For this purpose, we introduce a QD described by the confinement potential

$$V_{\mathrm{QD}} = -V_{\mathrm{QD}}\ \mathrm{sech}\left(\frac{|\mathbf{r}-\mathbf{r}_0|}{a_{\mathrm{QD}}}\right), \tag{2}$$

describing a QD centered at $\mathbf{r}_0$ with depth $V_{\mathrm{QD}} = 20$ meV and size parameter $a_{\mathrm{QD}} = 3$ nm. Such a QD has a single bound state with energy $\epsilon_1 \approx -7.6$ meV independently of $\mathbf{r}_0$ (when the latter is big enough to avoid overlapping with the barrier, as it is the case here). The wave function of this bound state has a full width at half maximum (FWHM) of approximately 7 nm and is in good agreement with the wave function of a cylindrical potential well with a diameter of about 10 nm. This state can be populated by capturing carriers from the 2D states via interaction with phonons [16, 26, 28]. In the $MoSe_2$ system at low temperature, the capture of conduction-band electrons takes place mostly via the emission of longitudinal optical (LO) phonons [28] with energy $E_{\mathrm{LO}} = 34.4\mathrm{meV} \approx E_0 - \epsilon_1$. In view of the dynamics shown in figure 1, the QD will be crossed by a different amount of charge depending on its position $\mathbf{r}_0$. To study the detection capability of the QD, we will compare the time-integrated density $\bar{n}(\mathbf{r})$ with the charge trapped in the QD at position $\mathbf{r}_0$ after the carrier capture. This is given by the quantity

$$f(\mathbf{r}_0) = \sum_{\alpha=1}^{N_b} f_\alpha \Big|_{\mathrm{QD\ in\ }\mathbf{r}_0;T\gg t_0+\tau}, \tag{3}$$

with N_b being in general the number of bound states of the QD (for our QD we have $N_b = 1$) and $f_\alpha|_T$ being the population of bound state α at time T after the wave packet has crossed the QD area. In previous works [26, 28] we have shown that the carrier capture shows an interesting time evolution and the capture takes place only in a finite time-window. Therefore, the final captured density $f_\alpha|_T$ is a well defined quantity for every T after this time-window. Thus, even if the readout of the occupation occurs in a time-integrated way, the signal provides information on the dynamics of the wave packet during a short time interval when it is in the region of the QD.

To describe the spatio-temporal carrier dynamics including the interaction with phonons, we use a recently introduced Lindblad single-particle approach within the density matrix formalism [26, 28]. It has been shown that this is a Markovian and trace-preserving [15, 61–64] description of carrier capture. The method is able to catch the locality of the scattering, while remaining computationally lighter than, e.g. full quantum kinetic equations [16, 26]. Details of the method can be found in [26, 28]. The resulting equations of motion for the density matrix elements are numerically integrated by standard finite time-difference techniques.

Figure 2(a) shows the captured density $f(\mathbf{r}_0)$ as function of the QD center at $x_0 = 50$ nm and varying y_0 (see vertical dashed line in figure 1(c)). For comparison we also show the time-integrated electron density $\bar{n}(\mathbf{r})$ at $x = x_0 = 50$ nm and

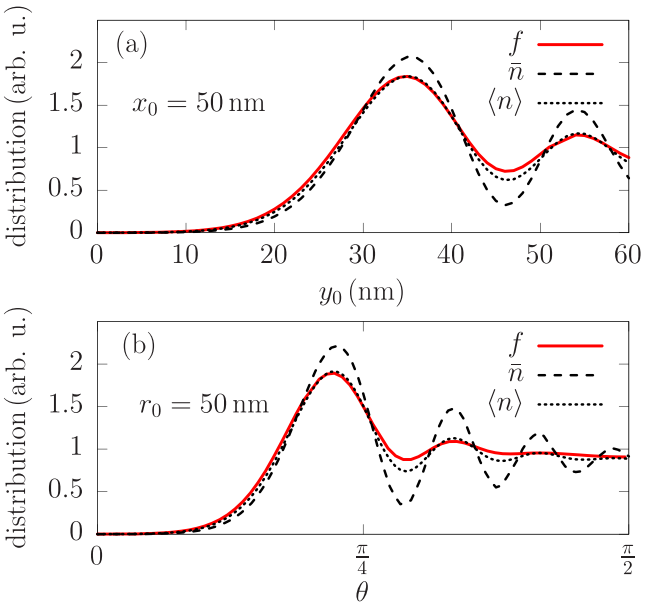

Figure 2. Captured electron density $f(\mathbf{r}_0)$ (solid line), time-integrated electronic density $\bar{n}(\mathbf{r})$ (dashed line) and averaged electronic density $\langle n\rangle(\mathbf{r}_0)$ for (a) fixed distance $x_0 = 50$ nm and (b) fixed radial distance $(r_0\cos\theta, r_0\sin\theta)$ with $r_0 = 50$ nm.

$y = y_0$. Both functions have been normalized to their center of the oscillations defined by the average between the second maximum and minimum. The agreement between these two curves is very good with $f(\mathbf{r}_0)$ being able to predict the locations of all the fringes displayed by $\bar{n}(\mathbf{r})$. A major difference is the amplitude of the spatial oscillations, which in the capture-induced results of $f(\mathbf{r}_0)$ are smaller than in the exact case of $\bar{n}(\mathbf{r})$. This deviation originates mostly from the character of the two quantities: while $\bar{n}(\mathbf{r})$ is defined at every single point $\mathbf{r}$, the bound state of the QD has a finite extension, therefore monitoring the density over an extended area. In order to show the contribution of the finite size of the receiving bound state, we consider the spatially averaged density

$$\langle n\rangle(\mathbf{r}_0) = \int \mathrm{d}\mathbf{r}\, \bar{n}(\mathbf{r})|\psi_1(\mathbf{r}-\mathbf{r}_0)|^2, \tag{4}$$

i.e. we coarse grain $\bar{n}(\mathbf{r})$ by the squared modulus of the receiving bound-state wave function ψ_1. The resulting spatially averaged density $\langle n\rangle(\mathbf{r}_0)$ is shown alongside $\bar{n}(\mathbf{r})$ and $f(\mathbf{r}_0)$ in figure 2(a). Note that $\langle n\rangle(\mathbf{r}_0)$ is normalized by the same factor as $\bar{n}(\mathbf{r})$. The oscillations of $\langle n\rangle(\mathbf{r}_0)$ now have a reduced amplitude very similar to the one of $f(\mathbf{r}_0)$, thus confirming that it is the size of the receiving state which mostly rules the magnitude of the signal provided by the capture-induced experiment. Larger QDs would therefore result in a loss of spatial resolution such that fringes of higher order become less visible. We nevertheless expect that especially the first fringe would still be well separated from the rest of the signal.

To experimentally realize such a set-up this would require movable QDs, which could in principle be created, e.g. by charged tips exploiting the so-called tip-induced band bending [65–67]. Such tip-induced QDs have been created for several years [68–70], resulting in the creation of zero-dimensional confinement potentials few tens of nanometers wide and few

tens of meV deep [70], resulting in a deepest bound state with FWHM of about 10 nm, i.e. not far from the FWHM of about 7 nm of the bound state ψ_1 here considered. We therefore expect that the reported spatial resolution can be achieved experimentally. Although mostly studied through electrical scanning-tunneling spectroscopy measurements, these tip-induced QDs could also be studied optically by putting a proper material under the studied surface [71, 72].

Another option to change the geometrical set-up is to keep the distance between the barrier and the QD fixed and rotate the sample by an angle θ around the barrier w.r.t. the incoming wave packet. In such a configuration the shape of the wave packet and the positioning of barrier and QD stay fixed. The corresponding results then lie on a circle with $\mathbf{r}_0 \equiv (r_0 \cos\theta, r_0 \sin\theta)$ and r_0 is the fixed distance between barrier and QD (see dashed-dotted line in figure 1(c)). The captured density $f(\mathbf{r}_0)$ in comparison to the exact results $\bar{n}(\mathbf{r})$ and the averaged density $\langle n \rangle(\mathbf{r}_0)$ for the rotation set-up are shown in figure 2(b). At larger angles the captured electron density $f(\mathbf{r}_0)$ is not able to efficiently address the location of the fringes anymore, because their amplitude and separation (see figure 1(c)) become too small to overcome the previously-described weakening of the amplitude. Nevertheless, as far as one considers bigger peaks, also in the case of figure 2(b) the matching is high, showing that our detection scheme can be performed also without movable QDs.

4. Conclusions

In conclusion, we have proposed a detection method to resolve the nanometer scale electron dynamics in a 2D system. For this purpose we have exploited the phonon-induced carrier capture into the bound states of a QD and shown the efficiency of the relation between exact and captured dynamics. In view of the developments of experimental techniques able to create movable QDs, we believe that the results reported here pave the way to an efficient detection of the spatio-temporal dynamics of low-energy carriers in 2D materials.

Acknowledgments

FL and DER acknowledge financial support from the Deutsche Forschungsgemeinschaft via the Project No. RE4183/2-1.

ORCID iDs

R Rosati https://orcid.org/0000-0002-2514-3425
F Lengers https://orcid.org/0000-0002-9571-4297
D E Reiter https://orcid.org/0000-0002-3648-353X
T Kuhn https://orcid.org/0000-0001-7449-9287

References

[1] Mohammed O F, Yang D-S, Pal S K and Zewail A H 2011 4D scanning ultrafast electron microscopy: visualization of materials surface dynamics *J. Am. Chem. Soc.* **133** 7708–11
[2] Yoshida S, Terada Y, Oshima R, Takeuchi O and Shigekawa H 2012 Nanoscale probing of transient carrier dynamics modulated in a GaAs–PIN junction by laser-combined scanning tunneling microscopy *Nanoscale* **4** 757–61
[3] Gabriel M M, Kirschbrown J R, Christesen J D, Pinion C W, Zigler D F, Grumstrup E M, Mehl B P, Cating E E, Cahoon J F and Papanikolas J M 2013 Direct imaging of free carrier and trap carrier motion in silicon nanowires by spatially-separated femtosecond pump–probe microscopy *Nano Lett.* **13** 1336–40
[4] Fukumoto K, Onda K, Yamada Y, Matsuki T, Mukuta T, Tanaka S-I and Koshihara S-Y 2014 Femtosecond time-resolved photoemission electron microscopy for spatiotemporal imaging of photogenerated carrier dynamics in semiconductors *Rev. Sci. Instrum.* **85** 083705
[5] Satoh T, Terui Y, Moriya R, Ivanov B A, Ando K, Saitoh E, Shimura T and Kuroda K 2012 Directional control of spin-wave emission by spatially shaped light *Nat. Photon.* **6** 662
[6] Brixner T, García de Abajo F J, Schneider J and Pfeiffer W 2005 Nanoscopic ultrafast space-time-resolved spectroscopy *Phys. Rev. Lett.* **95** 093901
[7] Wan Y, Guo Z, Zhu T, Yan S, Johnson J and Huang L 2015 Cooperative singlet and triplet exciton transport in tetracene crystals visualized by ultrafast microscopy *Nat. Chem.* **7** 785
[8] Man M K *et al* 2017 Imaging the motion of electrons across semiconductor heterojunctions *Nat. Nanotechnol.* **12** 36
[9] Guo Z, Wan Y, Yang M, Snaider J, Zhu K and Huang L 2017 Long-range hot-carrier transport in hybrid perovskites visualized by ultrafast microscopy *Science* **356** 59–62
[10] Liao B, Zhao H, Najafi E, Yan X, Tian H, Tice J, Minnich A J, Wang H and Zewail A H 2017 Spatial-temporal imaging of anisotropic photocarrier dynamics in black phosphorus *Nano Lett.* **17** 3675–80
[11] Kulig M, Zipfel J, Nagler P, Blanter S, Schüller C, Korn T, Paradiso N, Glazov M M and Chernikov A 2018 Exciton diffusion and halo effects in monolayer semiconductors *Phys. Rev. Lett.* **120** 207401
[12] Steininger F, Knorr A, Stroucken T, Thomas P and Koch S W 1996 Dynamic evolution of spatiotemporally localized electronic wave packets in semiconductor quantum wells *Phys. Rev. Lett.* **77** 550–3
[13] Pasenow B, Reichelt M, Stroucken T, Meier T and Koch S W 2005 Excitonic wave packet dynamics in semiconductor photonic-crystal structures *Phys. Rev.* B **71** 195321
[14] Reichelt M and Meier T 2009 Shaping the spatiotemporal dynamics of the electron density in a hybrid metal-semiconductor nanostructure *Opt. Lett.* **34** 2900–2
[15] Rosati R, Dolcini F and Rossi F 2015 Dispersionless propagation of electron wavepackets in single-walled carbon nanotubes *Appl. Phys. Lett.* **106** 243101
[16] Reiter D, Glanemann M, Axt V M and Kuhn T 2006 Controlling the capture dynamics of traveling wave packets into a quantum dot *Phys. Rev.* B **73** 125334
[17] Ferreira R and Bastard G 1999 Phonon-assisted capture and intradot Auger relaxation in quantum dots *Appl. Phys. Lett.* **74** 2818–20
[18] Magnusdottir I, Bischoff S, Uskov A V and Mørk J 2003 Geometry dependence of Auger carrier capture rates into cone-shaped self-assembled quantum dots *Phys. Rev.* B **67** 205326
[19] Markus A and Fiore A 2004 Modeling carrier dynamics in quantum-dot lasers *Phys. Status Solidi* a **201** 338–44
[20] Nielsen T R, Gartner P and Jahnke F 2004 Many-body theory of carrier capture and relaxation in semiconductor quantum-dot lasers *Phys. Rev.* B **69** 235314
[21] Seebeck J, Nielsen T R, Gartner P and Jahnke F 2005 Polarons in semiconductor quantum dots and their role

in the quantum kinetics of carrier relaxation *Phys. Rev.* B **71** 125327
[22] Trumm S, Wesseli M, Krenner H J, Schuh D, Bichler M, Finley J J and Betz M 2005 Spin-preserving ultrafast carrier capture and relaxation in InGaAs quantum dots *Appl. Phys. Lett.* **87** 153113
[23] Mielnik-Pyszczorski A, Gawarecki K and Machnikowski P 2015 Phonon-assisted tunneling of electrons in a quantum well/quantum dot injection structure *Phys. Rev.* B **91** 195421
[24] Ferreira R and Bastard G 2016 *Capture and Relaxation in Self-Assembled Semiconductor Quantum Dots* (San Rafael, CA: Morgan & Claypool)
[25] Reiter D, Glanemann M, Axt V M and Kuhn T 2007 Spatiotemporal dynamics in optically excited quantum wire-dot systems: capture, escape, and wave-front dynamics *Phys. Rev.* B **75** 205327
[26] Rosati R, Reiter D E and Kuhn T 2017 Lindblad approach to spatiotemporal quantum dynamics of phonon-induced carrier capture processes *Phys. Rev.* B **95** 165302
[27] Lengers F, Rosati R, Kuhn T and Reiter D E 2017 Spatio-temporal dynamics of carrier capture processes: simulation of optical signals *Acta Phys. Pol.* A **132** 372
[28] Rosati R, Lengers F, Reiter D E and Kuhn T 2018 Spatial control of carrier capture in two-dimensional materials: beyond energy selection rules *Phys. Rev.* B **98** 195411
[29] Glanemann M, Axt V M and Kuhn T 2005 Transport of a wave packet through nanostructures: quantum kinetics of carrier capture processes *Phys. Rev.* B **72** 045354
[30] Guenther T, Lienau C, Elsaesser T, Glanemann M, Axt V M, Kuhn T, Eshlaghi S and Wieck A D 2002 Coherent nonlinear optical response of single quantum dots studied by ultrafast near-field spectroscopy *Phys. Rev. Lett.* **89** 057401
[31] Sotier F, Thomay T, Hanke T, Korger J, Mahapatra S, Frey A, Brunner K, Bratschitsch R and Leitenstorfer A 2009 Femtosecond few-fermion dynamics and deterministic single-photon gain in a quantum dot *Nat. Phys.* **5** 352
[32] Mak K F and Shan J 2016 Photonics and optoelectronics of 2D semiconductor transition metal dichalcogenides *Nat. Photon.* **10** 216
[33] Wang Q H, Kalantar-Zadeh K, Kis A, Coleman J N and Strano M S 2012 Electronics and optoelectronics of two-dimensional transition metal dichalcogenides *Nat. Nano.* **7** 699
[34] Moody G *et al* 2015 Intrinsic homogeneous linewidth and broadening mechanisms of excitons in monolayer transition metal dichalcogenides *Nat. Commun.* **6** 8315
[35] Selig M, Berghäuser G, Raja A, Nagler P, Schüller C, Heinz T F, Korn T, Chernikov A, Malic E and Knorr A 2016 Excitonic linewidth and coherence lifetime in monolayer transition metal dichalcogenides *Nat. Commun.* **7** 13279
[36] Wang G, Chernikov A, Glazov M M, Heinz T F, Marie X, Amand T and Urbaszek B 2018 Colloquium: excitons in atomically thin transition metal dichalcogenides *Rev. Mod. Phys.* **90** 021001
[37] Mueller T and Malic E 2018 Exciton physics and device application of two-dimensional transition metal dichalcogenide semiconductors *npj 2D Mater. Appl.* **2** 29
[38] Guazzotti S, Pusch A, Reiter D E and Hess O 2018 Dynamic theory of nanophotonic control of two-dimensional semiconductor nonlinearities *Phys. Rev.* B **98** 245307
[39] Steinleitner P, Merkl P, Nagler P, Mornhinweg J, Schüller C, Korn T, Chernikov A and Huber R 2017 Direct observation of ultrafast exciton formation in a monolayer of WSe_2 *Nano Lett.* **17** 1455
[40] Steinhoff A, Florian M, Rösner M, Schönhoff G, Wehling T O and Jahnke F 2017 Exciton fission in monolayer transition metal dichalcogenide semiconductors *Nat. Commun.* **8** 1166
[41] Kumar S, Kaczmarczyk A and Gerardot B D 2015 Strain-induced spatial and spectral isolation of quantum emitters in mono-and bilayer WSe_2 *Nano Lett.* **15** 7567–73
[42] Tonndorf P, Schmidt R, Schneider R, Kern J, Buscema M, Steele G A, Castellanos-Gomez A, van der Zant H S J, de Vasconcellos S M and Bratschitsch R 2015 Single-photon emission from localized excitons in an atomically thin semiconductor *Optica* **2** 347–52
[43] Branny A, Wang G, Kumar S, Robert C, Lassagne B, Marie X, Gerardot B D and Urbaszek B 2016 Discrete quantum dot like emitters in monolayer $MoSe_2$: spatial mapping, magneto-optics, and charge tuning *Appl. Phys. Lett.* **108** 142101
[44] Krustok J *et al* 2016 Optical study of local strain related disordering in CVD-grown $MoSe_2$ monolayers *Appl. Phys. Lett.* **109** 253106
[45] Kern J *et al* 2016 Nanoscale positioning of single-photon emitters in atomically thin WSe_2 *Adv. Mater.* **28** 7101–5
[46] Branny A, Kumar S, Proux R and Gerardot B D 2017 Deterministic strain-induced arrays of quantum emitters in a two-dimensional semiconductor *Nat. Commun.* **8** 15053
[47] Palacios-Berraquero C, Kara D M, Montblanch A R-P, Barbone M, Latawiec P, Yoon D, Ott A K, Loncar M, Ferrari A C and Atatüre M 2017 Large-scale quantum-emitter arrays in atomically thin semiconductors *Nat. Commun.* **8** 15093
[48] Brooks M and Burkard G 2018 Theory of strain-induced confinement in transition metal dichalcogenide monolayers *Phys. Rev.* B **97** 195454
[49] Freitag N M *et al* 2016 Electrostatically confined monolayer graphene quantum dots with orbital and valley splittings *Nano Lett.* **16** 5798–805
[50] Ugeda M M *et al* 2014 Giant bandgap renormalization and excitonic effects in a monolayer transition metal dichalcogenide semiconductor *Nat. Mater.* **1312** 1091–5
[51] de Raad G J, Bruls D M, Koenraad P M and Wolter J H 2002 Interplay between tip-induced band bending and voltage-dependent surface corrugation on GaAs(1 1 0) surfaces *Phys. Rev.* B **66** 195306
[52] Rasmussen F A andThygesen K S 2015 Computational 2D materials database: electronic structure of transition-metal dichalcogenides and oxides *J. Phys. Chem.* C **119** 13169–83
[53] Khatibi Z, Feierabend M, Selig M, Linderälv C, Erhart P and Malic E 2019 Impact of strain on the excitonic linewidth in transition metal dichalcogenides *2D Mater.* **6** 015015
[54] Groß H, Hamm J M, Tufarelli T, Hess O and Hecht B 2018 Near-field strong coupling of single quantum dots *Sci. Adv.* **4** eaar4906
[55] Kleemann M-E *et al* 2017 Strong-coupling of WSe_2 in ultra-compact plasmonic nanocavities at room temperature *Nat. Commun.* **8** 1296
[56] Betzig E, Trautman J K, Harris T D, Weiner J S and Kostelak R L 1991 Breaking the diffraction barrier: optical microscopy on a nanometric scale *Science* **251** 1468–70
[57] Emiliani V, Günther T, Intonti F, Richter A, Lienau C and Elsaesser T 1999 Spatially and temporally resolved near-field spectroscopy of single GaAs quantum wires *J. Phys.: Condens. Matter* **11** 5889
[58] Neuberth U, Walter L, von Freymann G, Don B D, Kalt H, Wegener M, Khitrova G and Gibbs H M 2002 Combining a scanning near-field optical microscope with a picosecond streak camera: statistical analysis of exciton kinetics in GaAs single-quantum wells *Appl. Phys. Lett.* **80** 3340–2
[59] Kern J *et al* 2015 Nanoantenna-enhanced lightmatter interaction in atomically thin WS_2 *ACS Photonics* **2** 1260–5
[60] Vasa P, Ropers C, Pomraenke R and Lienau C 2009 Ultra-fast nano-optics *Laser Photonics Rev.* **3** 483–507

[61] Taj D, Iotti R C and Rossi F 2009 Microscopic modeling of energy relaxation and decoherence in quantum optoelectronic devices at the nanoscale *Eur. Phys. J.* B **72** 305–22
[62] Rosati R, Iotti R C, Dolcini F and Rossi F 2014 Derivation of nonlinear single-particle equations via many-body Lindblad superoperators: a density-matrix approach *Phys. Rev.* B **90** 125140
[63] Rosati R and Rossi F 2013 Microscopic modeling of scattering quantum non-locality in semiconductor nanostructures *Appl. Phys. Lett.* **103** 113105
[64] Rosati R and Rossi F 2014 Scattering nonlocality in quantum charge transport: application to semiconductor nanostructures *Phys. Rev.* B **89** 205415
[65] Weimer M, Kramar J and Baldeschwieler J D 1989 Band bending and the apparent barrier height in scanning tunneling microscopy *Phys. Rev.* B **39** 5572–5
[66] Feenstra R M, Dong Y, Semtsiv M and Masselink W 2006 Influence of tip-induced band bending on tunnelling spectra of semiconductor surfaces *Nanotechnology* **18** 044015
[67] Battisti I, Fedoseev V, Bastiaans K M, de la Torre A, Perry R S, Baumberger F and Allan M P 2017 Poor electronic screening in lightly doped Mott insulators observed with scanning tunneling microscopy *Phys. Rev.* B **95** 235141
[68] Dombrowski R, Steinebach C, Wittneven C, Morgenstern M and Wiesendanger R 1999 Tip-induced band bending by scanning tunneling spectroscopy of the states of the tip-induced quantum dot on InAs(1 1 0) *Phys. Rev.* B **59** 8043–8
[69] Morgenstern M, Haude D, Gudmundsson V, Wittneven C, Dombrowski R and Wiesendanger R 2000 Origin of Landau oscillations observed in scanning tunneling spectroscopy on n-InAs(1 1 0) *Phys. Rev.* B **62** 7257–63
[70] Morgenstern M, Gudmundsson V, Dombrowski R, Wittneven C and Wiesendanger R 2001 Nonlocality of the exchange interaction probed by scanning tunneling spectroscopy *Phys. Rev.* B **63** 201301
[71] Kemerink M, Sauthoff K, Koenraad P M, Gerritsen J W, van Kempen H, Fomin V M, Wolter J H and Devreese J T 2001 Optical properties of a tip-induced quantum dot *Appl. Phys.* A **72** 239
[72] Croitoru M D, Gladilin V N, Fomin V M, Devreese J T, Kemerink M, Koenraad P M, Sauthoff K and Wolter J H 2004 Electroluminescence spectra of an STM-tip-induced quantum dot *Physica* E **21** 2